



Interaction mechanism of ferrate(VI) with arsenopyrite surface and its effect on flotation separation of chalcopyrite from arsenopyrite

Run-peng LIAO^{1,2}, Pan-jin HU^{1,2}, Shu-ming WEN^{1,2}, Yong-xing ZHENG¹, Xian-hui QIU^{1,3}, Jin-fang LÜ^{1,2}, Jian LIU^{1,2}

1. State Key Laboratory of Complex Nonferrous Metal Resources Clean Utilization,
Kunming University of Science and Technology, Kunming 650093, China;

2. Faculty of Land Resource Engineering, Kunming University of Science and Technology, Kunming 650093, China;

3. Faculty of Resource and Environmental Engineering,

Jiangxi University of Science and Technology, Ganzhou 341000, China

Received 14 September 2021; accepted 6 January 2022

Abstract: Potassium ferrate (K_2FeO_4) was used as a novel environmental-friendly depressant, and its inhibition effect on flotation performance of arsenopyrite and chalcopyrite using potassium ethyl xanthate (PEX) as a collector was investigated by flotation experiments, contact angle measurements, adsorption measurements, localized electrochemical impedance spectroscopy (LEIS) measurements, and X-ray photoelectron spectroscopy (XPS) analyses. The results showed that K_2FeO_4 strongly depressed arsenopyrite in a pH range of 4–11, and the flotation separation of chalcopyrite from arsenopyrite could be realized in the presence of 5×10^{-4} mol/L K_2FeO_4 and 5×10^{-5} mol/L PEX at pH 8 or 10. In the presence of K_2FeO_4 and PEX, the contact angle and the xanthate adsorption capacity of arsenopyrite decreased significantly. LEIS measurements showed that the addition of ferrate could significantly increase the impedance of the arsenopyrite surface. XPS analyses further confirmed that ferrate accelerated the oxidation of arsenopyrite surface.

Key words: ferrate(VI); arsenopyrite; chalcopyrite; low-alkalinity flotation separation

1 Introduction

As an important strategic metal, copper plays a critical role in the social and economic development [1,2]. Chalcopyrite is the primary material source of copper in nature, and it is mainly recovered by flotation at present [3,4]. However, in common situations, chalcopyrite is closely associated with arsenopyrite, pyrite, and galena [5–7]. These minerals are close to chalcopyrite in ore-forming conditions, and some of their physical and chemical properties are also similar. Therefore, it is difficult to effectively separate these minerals by adding a single xanthate collector in the flotation process [2,8]. It is well known that Cu–As sulfide

ore is categorized into a complex refractory resource [9]. If chalcopyrite and arsenopyrite, as the main components, are not effectively separated in the flotation process, it will have adverse effects on the subsequent smelting process [10].

In the flotation separation of chalcopyrite from arsenopyrite, chalcopyrite and arsenopyrite show similar floatability because of the activation of copper ions on arsenopyrite surface [3,11]. Therefore, the separation of copper–arsenic sulfide ore by flotation depends on effective collectors and depressants, and the removal of arsenic from copper sulfide minerals by flotation has been extensively investigated with various approaches [12]. At present, xanthate is still the most widely used collector in the flotation of sulfide ore, and the main

products on the arsenopyrite surface are dixanthogens and arsenic(III) xanthates [13–15]. In recent years, O-isopropyl-N-ethyl thionocarbamate and N-butoxycarbonyl-O-isobutyl thiocarbamate have been used in flotation separation of chalcopyrite from arsenopyrite because of their higher selectivity to chalcopyrite [6,16,17]. Oxidation is usually viewed as an effective method to depress sulfide minerals. This is accounted by the fact that the formation of a hydrophilic layer, which consists of oxides or hydroxides, prevents xanthate adsorption on the surface of sulfide minerals [18,19]. Arsenopyrite is easily depressed at a high pH in the absence or presence of oxidants [20]. However, there are inevitable problems in high-alkaline process, such as pipeline scaling, low recovery rate of associated precious metals, difficulty in beneficiation wastewater treatment. Aeration conditioning was considered to be effective in pre-oxidation. The arsenic and iron in the arsenopyrite are more reactive than iron in the chalcopyrite, indicating that arsenopyrite is easily depressed at a high pH during flotation [21–24]. Thus, aeration represents the most simple and effective method for depression of arsenopyrite [25]. In addition, pre-oxidation by using oxidizing agents, including hydrogen peroxide, manganese dioxide, potassium permanganate, and hypochlorous acid, has been used to inhibit flotation of the arsenopyrite [20,22,26–29].

Ferrate(VI) is a powerful oxidant in the whole pH range. Compared with potassium permanganate and other oxides, the oxidation of ferrate is stronger. The standard electrode potential is 0.72 V under an alkaline condition and 2.20 V under an acidic condition [30,31]. High selectivity can be achieved by adjusting the pH value [32]. It has many advantages such as high stability, and non-toxic and harmless reaction products. Thus, it is widely used in sewage treatment and environmental remediation [33,34]. The strong oxidation of ferrate(VI) can oxidize the arsenopyrite surface and meanwhile, the ferrate(VI) is reduced into Fe(III). In an alkaline solution, considerable amounts of hydroxyl iron will adsorb on the arsenopyrite surface, which provides sufficient possibility to reduce the hydrophobicity of arsenopyrite surface [35].

In this study, a novel depressant was proposed for selectively depressing arsenopyrite to achieve

the flotation separation of chalcopyrite from arsenopyrite. Effects of ferrate(VI) on the Cu–As sulfides flotation separation performances were studied by flotation tests. The inhibition mechanism of arsenopyrite by ferrate(VI) was investigated by the contact angle, surface adsorption experiments, localized electrochemical impedance spectroscopy measurements (LEIS), and X-ray photoelectron spectroscopy (XPS). It is believed that the present study will lay an excellent foundation for selecting an effective depressant during flotation of Cu–As sulfide ores.

2 Experimental

2.1 Materials

Chalcopyrite and arsenopyrite with high purity were obtained from Chifeng, Inner Mongolia, China. Gangue minerals were artificially removed from high-grade chalcopyrite and arsenopyrite and then were hand-picked, crushed, dry ground and screened. A particle size range of 45–75 μm was used for flotation tests, surface-adsorption measurements and XPS measurements. The polished lump mineral was used for contact angle and LEIS measurements. Chemical analysis showed that chalcopyrite samples contain 33.28% copper, and arsenopyrite samples contain 45.12% arsenic. XRD analysis results of chalcopyrite and arsenopyrite were obtained by using the MDI Jade 6.0 Package, as shown in Fig. 1. It is seen that there are few diffraction peaks of gangue minerals in both samples, which can be used for pure mineral flotation and mechanism investigation.

As one kind of ferrate(VI), potassium ferrate with an analytical purity was employed as a depressant. Potassium ethyl xanthate (PEX) and pine oil, which were of industrial purity, were used as collector and frother, respectively. In addition, hydrochloric acid and sodium hydroxide were used as pH regulators. Deionized water with a resistivity of 18.3 $\text{M}\Omega\cdot\text{cm}$ was used in all experiments.

2.2 Micro-flotation tests

An RK/FGC 5–35 trough-type flotation machine was used for micro-flotation tests. In the micro-flotation tests, approximately 2 g of pure mineral samples were initially treated with an ultrasonic cleaner for 5 min to remove the oxidized components from the mineral surface. The

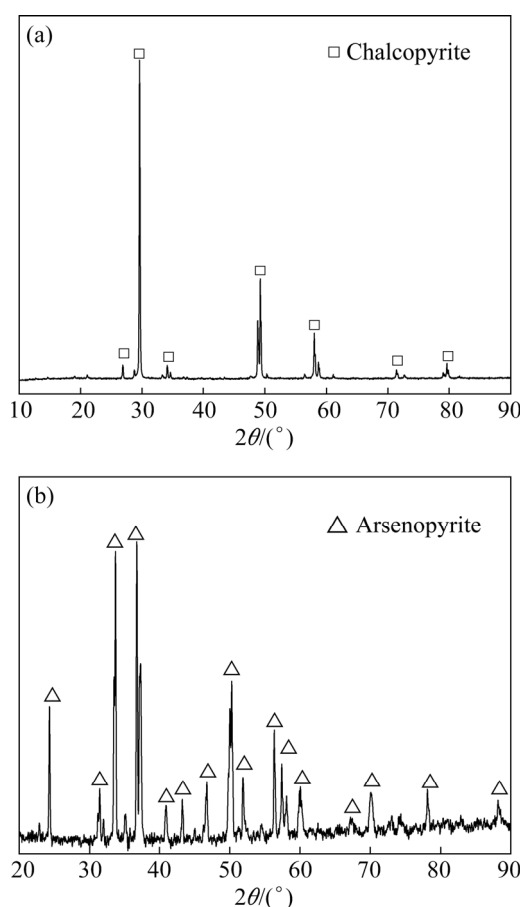


Fig. 1 XRD patterns of purified chalcopyrite (a) and arsenopyrite (b)

supernatant was removed and the mineral sample was mixed with deionized water and reagent to maintain the pulp volume of 40 mL. Then, the prepared pulp was added into the flotation cell at a stirring speed of 1600 r/min. The pH of pulp was measured by pH meter (PHS-3C, Wincom, China) and was adjusted by using hydrochloric acid and sodium hydroxide for 2 min. Ferrate(VI) solution was injected into the pulp, followed by addition of PEX (5×10^{-5} mol/L, 3 min) and pine oil (15 mg/L, 2 min). After flotation for 3 min, the single mineral recovery was calculated by weighing the concentrate and tailings. Recovery of the mineral mixture, which was composed of 1.0 g of chalcopyrite and 1.0 g of arsenopyrite, was calculated based on chemical assays of contents of copper and arsenic in the concentrate and tailing.

2.3 Contact angle measurements

Contact angle can characterize the surface wettability of chalcopyrite and arsenopyrite. A large block of mineral was cut into a rectangle

(1.0 cm \times 1.0 cm \times 0.2 cm) and then was polished with wet silicon carbide and aluminum oxide powder suspension. For the prepared chalcopyrite and arsenopyrite, four testing steps in the following orders were carried out: (1) Both the prepared samples were ultrasonically cleaned with deionized water and then were dried in a vacuum drying oven at 30 °C; (2) The dried samples were soaked in sodium hydroxide solution at pH 8.0 for 3 min; (3) Ferrate(VI) solution with a concentration of 2×10^{-4} mol/L was added and reacted for 5 min; (4) Finally, 5×10^{-5} mol/L PEX was added for 2 min. Video contact angle tester (JY-82B) was used to measure the contact angles of deionized water drops at the surface of chalcopyrite and arsenopyrite under different treatment conditions.

2.4 Surface adsorption experiments

Concentration of PEX in pulp was determined by ultraviolet–visible spectrophotometer (uv-2700) and adsorption concentration of PEX at the surface of chalcopyrite and arsenopyrite could be calculated. Approximately 2.0 g of samples each time were used for adsorption experiments, and the testing solution was prepared as follows. Firstly, the mineral was cleaned by ultrasound, mixed with 40 mL deionized water and then were stirred using a magnetic stirrer. Then, the pulp was adjusted to pH 8.0. After that, 2×10^{-4} mol/L ferrate(VI) and 5×10^{-5} mol/L PEX were added to the pulp for 5 and 3 min, respectively. Finally, the mixture was filtered and centrifuged, and about 15 mL of supernatant was taken for testing.

The calculation of adsorption capacity was described as follows:

$$\Gamma_M = \frac{(C_0 - C)V}{m} \quad (1)$$

where Γ_M (mol/g) is the adsorption concentration of PEX, C_0 (mol/L) is the initial concentration of PEX in pulp, C (mol/L) is the residual concentration of PEX in pulp, V (L) is the volume of pulp, and m (g) is the mass of mineral.

2.5 LEIS measurements

The polished flake arsenopyrite was fixed in a cylinder with a diameter of 3 cm by using epoxy resin. The sample was wiped with alcohol before testing. Then, the sample was immersed into 1×10^{-3} mol/L KCl solution. Finally, the impedance distribution of arsenopyrite surface before and after

treatment with ferrate(VI) was obtained by the micro scanning electrochemical test system (Versa STAT 3F, Ametek, America). The same was used in the test process, and the equipment probe scanned the same area to compare the impedance changes of mineral surface before and after potassium ferrate treatment. The scanning range was set as $800\ \mu\text{m} \times 800\ \mu\text{m}$ and the step size was set as $50\ \mu\text{m}$. The scanning frequency was kept at 1 kHz and the testing voltage was fixed to be 10 mV.

2.6 XPS analyses

The X-ray photoelectron spectroscopy was recorded using a scanning XPS microprobe system. Chemical composition and concentration variation of element at the arsenopyrite surface before and after interaction with ferrate(VI) were measured. Approximately 2 g of arsenopyrite samples were added into a beaker which was filled with 40 mL water and then the pulp was stirred in a magnetic stirrer based on the single mineral flotation process. These elements such as C 1s, O 1s, Fe 2p, S 2p and As 3d were focused on and the spectrum was calibrated on the basis of the C 1s peak at 284.8 eV. XPS analyses were carried out on a K-Alpha system, which is developed by Thermo Fisher Scientific. Curve was fitted using the Thermo Avantage software after narrow spectrum scanning at a pass-energy of 50 eV.

3 Results and discussion

3.1 Flotation

3.1.1 Single mineral flotation

Figure 2 shows the flotation recovery of chalcopyrite and arsenopyrite as a function of ferrate(VI) dosage at pH 8.0 and a PEX concentration of $5 \times 10^{-5}\ \text{mol/L}$. As shown in Fig. 2, chalcopyrite and arsenopyrite showed a favorable floatability with a recovery of 93.19% and 78.70%, respectively, in the absence of ferrate(VI). The continuous increase in ferrate(VI) concentration had a slight effect on flotation recovery of chalcopyrite. Flotation recovery of chalcopyrite only decreased from 93.19% to 83.71% when ferrate(VI) dosage increased from 0 to $6 \times 10^{-4}\ \text{mol/L}$. However, the recovery of arsenopyrite obviously decreased from 78.70% to 20.30%. These results may be explained that arsenopyrite is more easily oxidized than chalcopyrite under the same conditions [36,37].

Therefore, it was concluded that the addition of ferrate(VI) could significantly increase floatability differences between chalcopyrite and arsenopyrite in the presence of PEX.

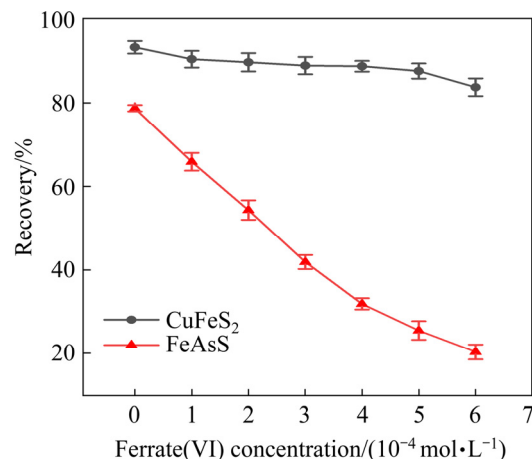


Fig. 2 Effects of ferrate(VI) concentration on flotation recovery of both minerals

Figure 3 presents the flotation recovery of chalcopyrite and arsenopyrite as a function of pH at a PEX concentration of $5 \times 10^{-5}\ \text{mol/L}$ before and after adding $5 \times 10^{-4}\ \text{mol/L}$ ferrate(VI). The chalcopyrite recovery curves showed the same trend before and after introducing ferrate(VI). Recovery of chalcopyrite fluctuated from 82.48% to 96.16% in the whole pH range in the absence of ferrate(VI), indicating that chalcopyrite had good floatability. Under high alkalinity conditions, the hydroxyl complex of iron was easy to be generated at the surface of chalcopyrite, which made the recovery of chalcopyrite slightly decrease [38,39]. After adding ferrate(VI) into the pulp, recovery of chalcopyrite only decreased by about 5% under various pH conditions, indicating that the chalcopyrite still had good floatability. For the flotation of arsenopyrite without addition of ferrate(VI), it had good flotation performances in pH range of 4.0–9.0, corresponding to their respective recovery of 92.23% and 74.95%. The mechanism was responsible for the formation of dixanthogen and arsenic(III) xanthates at the surface of arsenopyrite in the flotation system using xanthate as collector [14]. At a pH > 9.0, recovery of arsenopyrite rapidly decreased and the lowest recovery reached 6.47%. This was explained by the fact that the formed hydrophobic species were unstable and even could not adsorb on the surface of arsenopyrite [40]. After adding ferrate(VI) in a pH range of 4.0–11.0, the flotation recovery of

arsenopyrite significantly decreased. Flotation recovery of arsenopyrite decreased from 78.70% to 25.44% at pH 8.0. These results may be accounted by the fact that more hydrophilic products were adsorbed on the arsenopyrite surface, which reduced the adsorption of collector.

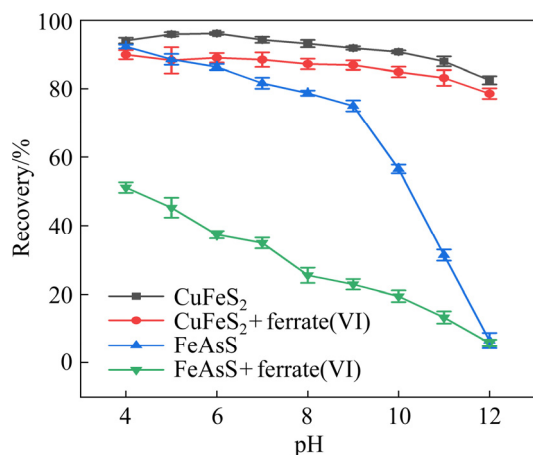


Fig. 3 Flotation performances of both minerals as function of pH

Effects of interaction time of ferrate(VI) on recovery of chalcopyrite and arsenopyrite were investigated at pH 8.0 and a PEX concentration of 5×10^{-5} mol/L before and after adding 5×10^{-4} mol/L ferrate(VI), as shown in Fig. 4. It is seen that the recovery of chalcopyrite slowly decreased with increasing in interaction time. When interaction time increased to 15 min, recovery of chalcopyrite was still as high as 79.71%. However, flotation recovery of arsenopyrite significantly decreased with increasing interaction time. When the interaction time increased to 5 min, the difference of concentrate recovery between arsenopyrite and chalcopyrite reached 59.87%. With a further increase in interaction time to 15 min, their difference of recovery increased to 68.68%. These results suggested that chalcopyrite could be effectively separated from arsenopyrite by prolonging interaction time of the depressant to form more oxidation products on the surface [41].

3.1.2 Mineral mixture flotation

To verify the selective inhibition of ferrate(VI) on arsenopyrite, flotation separation tests were carried out for the artificial mineral mixture. According to single mineral flotation results, the suitable flotation conditions of mineral mixture were determined as: initial pH range of 8.0–10.0, ferrate(VI) concentration of 5×10^{-4} mol/L and PEX

concentration of 5×10^{-5} mol/L. The flotation results are given in Table 1. It is seen that recovery of chalcopyrite in the concentrate reached 93.91% after flotation at pH 8.0 in the presence of ferrate(VI), which was nearly consistent with the single mineral flotation results. On the other hand, recovery of arsenopyrite reached 38.55%, which was slightly higher than that of arsenopyrite in single mineral flotation tests. This may be explained by the fact that copper ions that were released from the chalcopyrite were adsorbed on the surface of arsenopyrite [42]. When the pH increased to 10.0, recovery of arsenopyrite in the concentrate decreased to 22.06%, indicating that a satisfactory separation performance was achieved. Therefore, it was promising that ferrate(VI) was used to separate chalcopyrite from arsenopyrite under low alkalinity conditions.

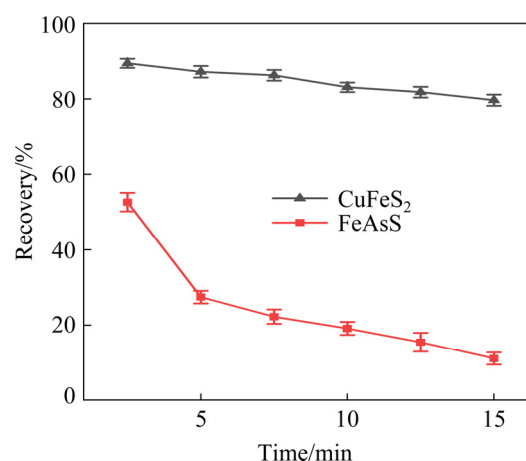


Fig. 4 Effect of interaction time of ferrate(VI) on recovery of both minerals

Table 1 Flotation results for mixture of chalcopyrite and arsenopyrite

pH	Product	Yield/%	Grade/%		Recovery/%	
			Cu	As	CuFeS ₂	FeAsS
8.0	Concentrate	64.54	23.80	13.58	93.91	38.55
	Tailing	35.46	2.81	39.41	6.09	61.45
	Feeding	100.00	16.36	22.74	100.00	100.00
10.0	Concentrate	54.12	26.50	8.92	91.04	22.06
	Tailing	45.88	3.21	38.81	8.96	77.94
	Feeding	100.00	15.82	22.63	100.00	100.00

3.2 Contact angle

To investigate the wettability of chalcopyrite and arsenopyrite under different conditions, contact

angle measurements were carried out and the results are shown in Fig. 5 and Table 2. Figure 5 shows the visual changes of contact angle after treating with different reagents. Table 2 shows that contact angles of the polished chalcopyrite and arsenopyrite after immersing in NaOH solution at pH 8.0 reached 64.48° (Fig. 5(a)) and 62.62° (Fig. 5(a1)), respectively. When ferrate(VI) was added, contact angles of chalcopyrite and arsenopyrite decreased by 12.91° (Fig. 5(b)) and 17.17° (Fig. 5(b1)), respectively. With a further introduction of PEX, contact angle of chalcopyrite increased from 51.57° to 60.91° (Fig. 5(c)), but contact angle of arsenopyrite decreased from 45.45° to 40.08° (Fig. 5(c1)). The latter may be explained by more hydrophilic substances produced at the surface of arsenopyrite after adding PEX [41]. The process of PEX interacting with arsenopyrite factually increased interaction time in contrast with no addition of PEX, which further supported the results obtained in Fig. 4. The difference of contact angle between chalcopyrite and arsenopyrite reached 20.83° in the flotation system, suggesting that chalcopyrite could be effectively separated from arsenopyrite.

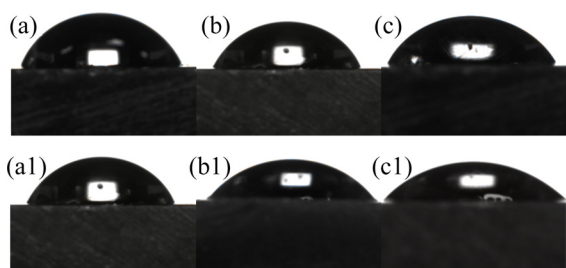


Fig. 5 Photographs of contact angle of chalcopyrite (a–c) and arsenopyrite (a1–c1) after treating under different conditions

Table 2 Contact angle of chalcopyrite and arsenopyrite after treating under different conditions

Condition	Contact angle/ $^\circ$	
	Chalcopyrite	Arsenopyrite
pH 8.0	64.48	62.62
pH 8.0 + ferrate(VI)	51.57	45.45
pH 8.0 + ferrate(VI) + PEX	60.91	40.08

3.3 Surface adsorption

Floatability of sulfide minerals in xanthate-induced flotation system mainly depends on the

adsorption capacity of xanthate on the mineral surface [43,44]. Therefore, effects of ferrate(VI) on adsorption of collectors at the surface of chalcopyrite and arsenopyrite were investigated and the results are shown in Fig. 6. The adsorption amounts of xanthate on the surface of chalcopyrite and arsenopyrite maintained high levels when there was no addition of ferrate(VI). After adding ferrate(VI), adsorption capacity of collector on chalcopyrite surface slightly decreased, whereas adsorption capacity of collector on arsenopyrite surface significantly decreased. When the concentration of ferrate(VI) increased from 0 to 5×10^{-4} mol/L, the adsorption amounts of xanthate on the surface of chalcopyrite and arsenopyrite decreased from 1×10^{-6} mol/g to 7.2×10^{-7} mol/g and from 7.6×10^{-7} mol/g to 1.2×10^{-7} mol/g, respectively, which further confirmed that ferrate(VI) could selectively oxidize arsenopyrite. With a further increase in concentration of ferrate(VI), both the adsorption amounts had little changes. These results further supported the results of flotation tests and contact angle measurements.

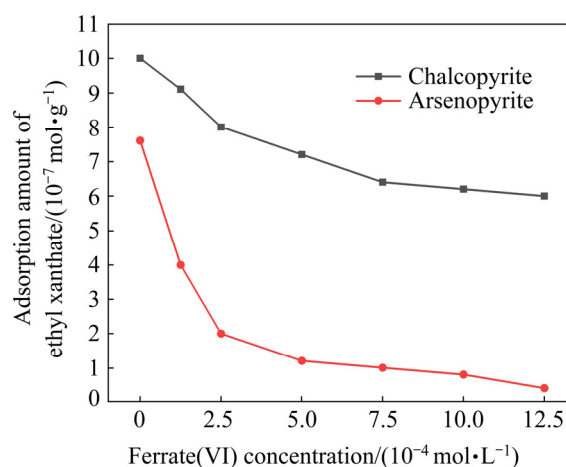


Fig. 6 Amounts of PEX adsorbed on surfaces of chalcopyrite and arsenopyrite as function of ferrate(VI) concentration

3.4 LEIS analyses

To further investigate depressing mechanisms of arsenopyrite, LEIS analyses were performed and the results are shown in Fig. 7. It is seen that the LEIS maps of arsenopyrite surfaces were dominated by green, yellow and red, which indicated that impedance values continuously increased. Thus, impedance value of arsenopyrite surface with addition of ferrate(VI) (Fig. 7(b)) was far higher than that of arsenopyrite surface without

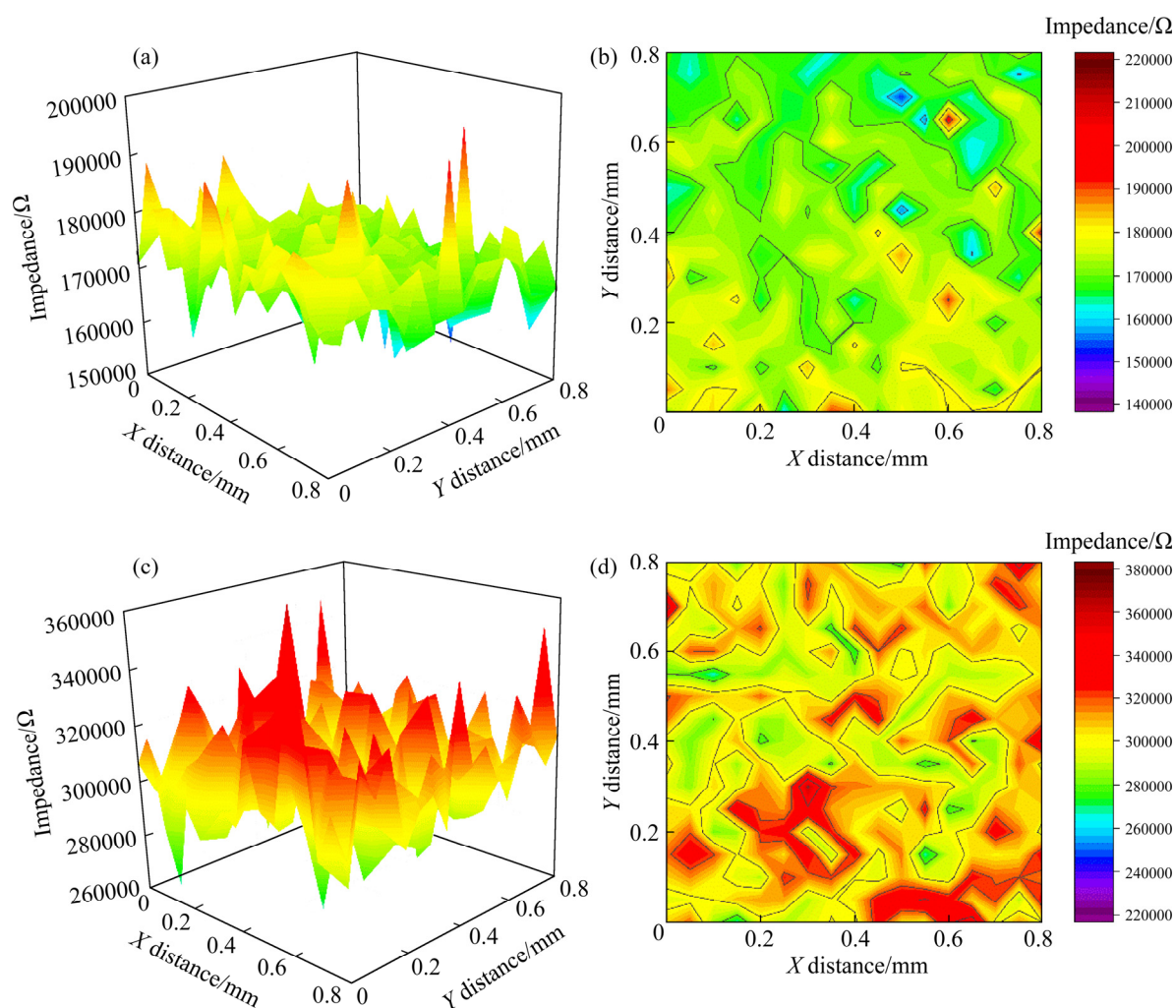


Fig. 7 LEIS maps of arsenopyrite surface without (a, b) and with (c, d) addition of ferrate(VI)

addition of ferrate(VI) (Fig. 7(b)). By calculating average value of the impedance value per unit area, the average impedance values of arsenopyrite samples before and after treating with ferrate(VI) were 172222.8 and 304216.2 Ω , respectively. This may be explained by the fact that a large number of iron oxides and arsenates with poor conductivity were produced on surface of arsenopyrite [41,45]. The formed products that were often characterized by hydrophilicity decreased the floatability of arsenopyrite, which further supported the results obtained in Sections 3.1–3.3.

3.5 XPS analyses

Figure 8 shows comprehensive XPS spectra of arsenopyrite without and with ferrate(VI). It can be seen that, there were no obvious changes of peak intensity. Table 3 presents the compositions of arsenopyrite surface without and with addition of

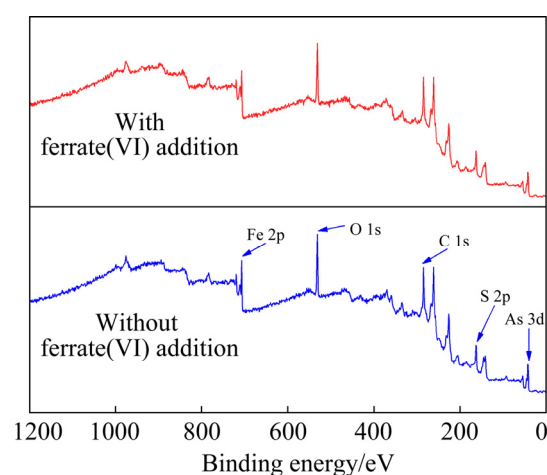


Fig. 8 Comprehensive XPS spectra of arsenopyrite without and with addition of ferrate(VI)

ferrate(VI). The molar fractions of O and Fe increased from 18.26% to 20.76% and from 6.62% to 8.38%, respectively, after adding ferrate(VI),

which indicated that more iron oxides or hydroxides were formed at the surface of arsenopyrite. In addition, there were little changes for molar fraction of S and As. Concentration changes of C atomic may be ascribed to carbon pollution [46].

Table 3 Compositions of arsenopyrite surface without and with addition of ferrate(VI)

Sample	Composition/at.%				
	O 1s	S 2p	Fe 2p	As 3d	C 1s
With ferrate(VI) addition	18.26	13.62	6.62	11.41	50.08
Without ferrate(VI) addition	20.76	12.87	8.38	11.55	46.44

Figure 9 shows the high-resolution XPS spectra of S 2p, As 3d, Fe 2p and O 1s for arsenopyrite surface without and with addition of ferrate(VI). Correspondingly, their assignment and properties are given in Tables 4–7. Figure 9(a) shows that S 2p XPS spectra were composed of a doublet structure of S 2p_{3/2} and S 2p_{1/2} levels. The

S 2p_{3/2} peak was only fitted due to the fact that the strength of S 2p_{3/2} is higher than that of S 2p_{1/2}. Curve fitting of the S 2p_{3/2} core level peak indicated that it was divided into three components. The peak, which was located at a binding energy of 161.41 or 161.52 eV, was assigned to S in the generated S²⁻ species (e.g. AsS₃³⁻) [47–49]. Another peak, which was centred at a binding energy of 162.39 or 162.48 eV, was contributed by S in arsenopyrite (FeAsS) [45,50]. The third at 163.76 or 163.88 eV was ascribed to S in polysulfides (S_n) [51]. The relative contents of S 2p_{3/2} for the both samples are presented in Table 4. These species, such as S²⁻ species and polysulfides, were generated at the surface of arsenopyrite due to the oxidation and adsorption before addition of ferrate(VI). After addition of ferrate(VI), the percentage of S in FeAsS decreased, whereas the percentage of S in S²⁻ species increased, indicating that S in FeAsS was reduced into S²⁻ [47]. Thus, the recovery of arsenopyrite decreased after adding ferrate(VI), as shown in Figs. 2–4.

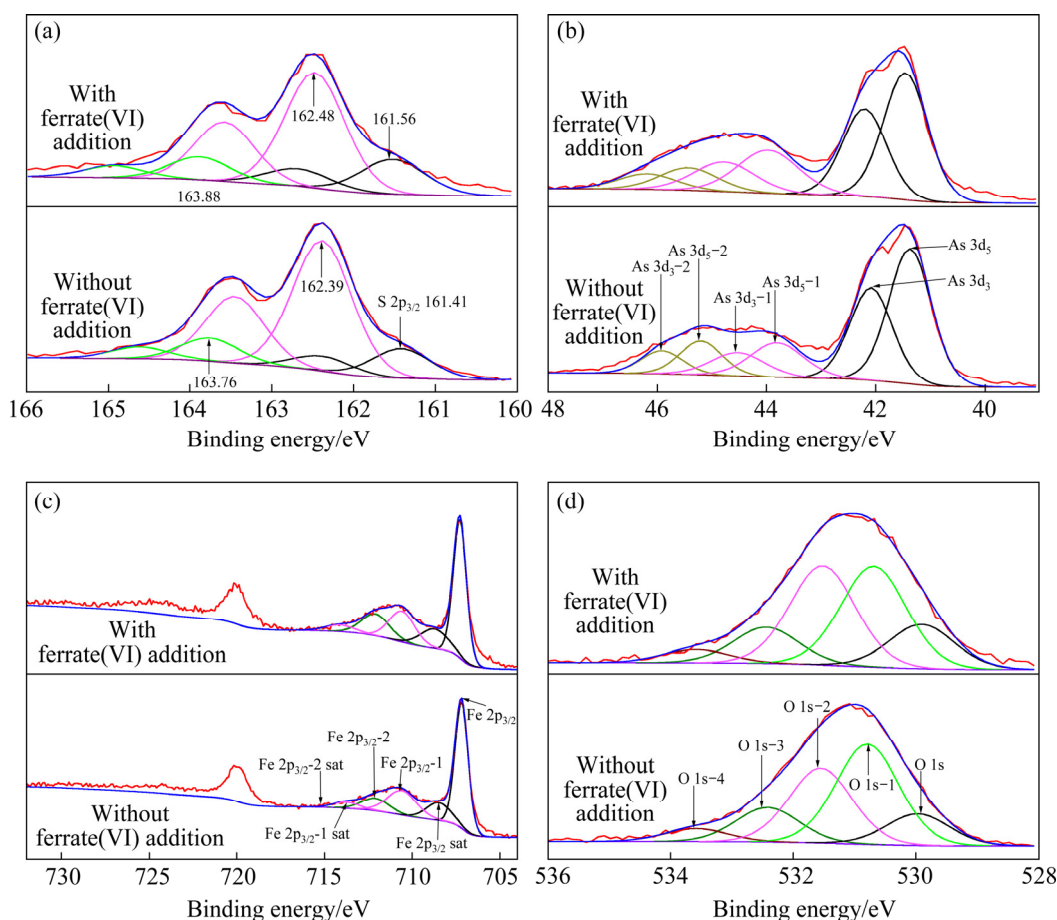


Fig. 9 High-resolution XPS spectra of S 2p (a), As 3d (b), Fe 2p (c) and O 1s (d) for arsenopyrite without and with addition of ferrate(VI)

Table 4 Assignment and properties of S 2p_{3/2} XPS spectra

Sample	Binding energy/eV			Molar fraction/%		
	S ²⁻	FeAsS	S _n	S ²⁻	FeAsS	S _n
Without ferrate(VI) addition	161.41	162.39	163.76	16.19	71.25	12.54
With ferrate(VI) addition	161.52	162.48	163.88	21.16	65.64	13.19

Table 5 Assignment and properties of As 3d_{5/2} XPS spectra

Sample	Binding energy/eV			Molar fraction/%		
	FeAsS	As(III)	As(V)	FeAsS	As(III)	As(V)
Without ferrate(VI) addition	41.38	43.81	45.20	63.53	20.55	15.91
With ferrate(VI) addition	41.46	43.97	45.43	59.06	27.37	13.57

Table 6 Assignment and properties of Fe 2p_{3/2} XPS spectra

Sample	Binding energy/eV			Molar fraction/%		
	FeAsS	Fe—O mixture	Scorodite	FeAsS	Fe—O mixture	Scorodite
Without ferrate(VI) addition	707.19	710.59	712.11	60.71	26.54	12.75
With ferrate(VI) addition	707.28	710.59	712.10	56.48	24.56	18.96

Table 7 Assignment and properties of O 1s XPS spectra

Sample	Binding energy/eV					Molar fraction/%				
	Iron oxides	C=O	OH ⁻	C—O	O=C—O	Iron oxides	C=O	OH ⁻	C—O	O=C—O
Without ferrate(VI) addition	529.97	530.79	531.55	532.42	533.58	12.45	39.37	29.43	13.65	5.09
With ferrate(VI) addition	529.90	530.69	531.52	532.44	533.58	14.97	34.35	33.83	12.30	4.53

O=C—O refers to the oxygen in the C—O single bond when a carbon in the organic pollutants is connected to a C—O single bond and a C=O double bond at the same time

According to Fig. 9(b), As 3d XPS spectra consisted of a doublet structure that represented the spin-orbit splitting of the As 3d_{5/2} and As 3d_{3/2}, and the peak area ratio is 2:1. Fitting results of As 3d_{5/2} peak showed three signals at 41.38 or 41.46 eV, 43.81 or 43.97 eV and 45.20 or 45.43 eV, which were ascribed to As in FeAsS [45,52], As(III) [49] and As(V) [45], respectively. Table 5 gives the assignment and properties of As 3d_{5/2} XPS spectra. Both As(III) and As(V) species were formed at the surface of arsenopyrite ascribed to its self oxidation and perceptive reactions before addition of ferrate(VI) [53]. After treating with ferrate(VI), the percentage of As in FeAsS decreased, but the percentage of As in As(III) species increased. According to fitting results of S 2p_{3/2} core peak, it was deduced that As(III) mainly existed in the form of AsS₃³⁻ species. Moreover, As in FeAsS was easily oxidized into As(III) and even As(V), which

gave rise to greater electron density associated with S in FeAsS, resulting in the increase in the percentage of S in S²⁻ species, as shown in Table 4.

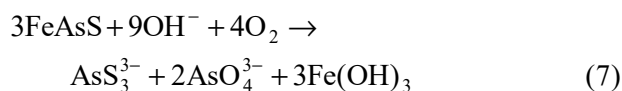
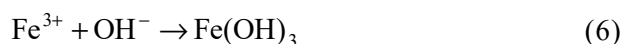
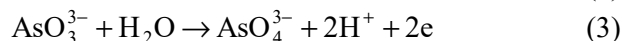
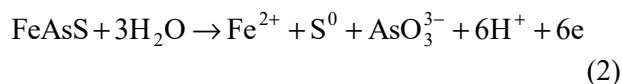
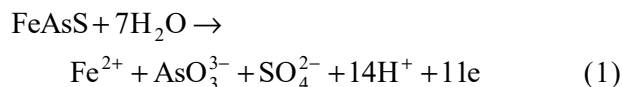
From Fig. 9(c), the Fe 2p peaks exhibited a spin-orbit doublet and the area ratio of Fe 2p_{3/2} to Fe 2p_{1/2} was 2:1. Therefore, only the Fe 2p_{3/2} component was considered for curve fitting. The Fe 2p_{3/2} component revealed three signals at 707.19 or 707.28 eV, 710.59 and 712.10 or 712.11 eV, respectively, which were assigned to Fe in FeAsS [54], mixtures of Fe₂O₃ and FeO [55,56] and Fe(III) species [45,54], respectively. Table 6 also shows that the percentage of Fe in FeAsS decreased, but the percentage of Fe in Fe(III) species increased after addition of ferrate(VI). According to fitting results of As 3d_{5/2} peak, it was deduced that Fe(III) mainly existed in the form of scorodite. These results were also verified by the fitting results of O 1s XPS spectra, as shown in Fig. 9(d) and Table 7.

It is seen that the fitting curves presented five components, which were separately located at average binding energies of 529.94, 530.74, 531.54, 532.43 and 533.58 eV. Correspondingly, they were contributed by O in iron oxides, C=O, Fe(OH)₃, C—O and O=C—O [46,56,57], respectively. It is also known that the percentage of O in iron oxides and Fe(OH)₃ increased after adding ferrate(VI), which further confirmed that impedance values of arsenopyrite surface increased after treating with ferrate(VI), as shown in Fig. 7.

3.6 Mechanism of ferrate(VI) depressing on arsenopyrite

According to the above results and discussion, schematic diagram of depression of ferrate(VI) on arsenopyrite surface during flotation was designed, as shown in Fig. 10. The arsenopyrite was initially oxidized into AsO₃³⁻ species and sulfur species, including polysulfides, elemental sulfur and even sulfates, with a high valence states by oxygen in the solution, as described in Eqs. (1) and (2). The generated AsO₃³⁻ and Fe²⁺ were further oxidized into AsO₄³⁻ and Fe³⁺, respectively, as described in Eqs. (3) and (4). When the arsenopyrite was immersed into a solution under alkaline condition, these oxidation reactions were accelerated, which generated more precipitates of ferric hydroxide and iron arsenate generate at the surface of arsenopyrite and in the solution, as described in Eqs. (5) and (6). In addition, As in FeAsS could be also oxidized into

thioarsenite (AsS₃³⁻) on the surface, as expressed by Eq. (7):



With a further introduction of ferrate(VI), a spontaneous decomposition reaction of Fe(VI) in solution forms molecular oxygen and Fe(III) (Eq. (8)). These products further oxidize the surface of arsenopyrite, resulting in more and more hydrophilic species formed. According to the XPS analyses results, the reactions of generation of ferric hydroxide (Eq. (6)) and AsS₃³⁻ (Eq. (7)) may be dominated after adding ferrate(VI). In addition, the dehydration of ferric hydroxide also occurred, as described by Eq. (9):

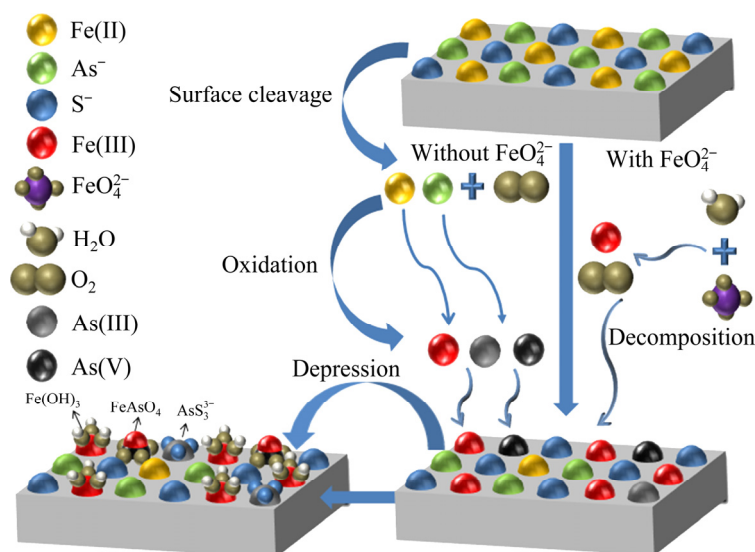
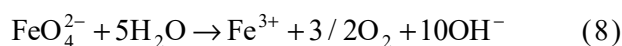


Fig. 10 Schematic diagram of depression of ferrate(VI) on arsenopyrite surface

4 Conclusions

(1) Ferrate(VI) significantly depressed arsenopyrite in a pH range of 4–11 for the single mineral flotation tests, but slightly depressed chalcopyrite. In mineral mixtures flotation tests, difference value of 55.36% for the both recovery was obtained at pH 8.0 after adding ferrate(VI). The difference value further increased to 68.98% with a further increase in pH, indicating that an excellent separation performance was achieved.

(2) Contact angles of arsenopyrite and chalcopyrite intensively and slightly decreased, respectively, after introducing ferrate(VI), which confirmed that an obvious difference of wettability occurred. Adsorption capacity of collector on arsenopyrite surface significantly decreased more than that of chalcopyrite after adding ferrate(VI), suggesting that discrepancy of hydrophobicity was enlarged.

(3) Impedance obviously increased in contrast with no addition of ferrate(VI), which illustrated that more iron oxides and arsenates with poor conductivity were produced. The formation of such hydrophilic species, including thioarsenite, scorodite, iron oxides and ferric hydroxides at the surface decreased the floatability.

Acknowledgments

This work was supported by the National Natural Science Foundation of China (Nos. 52074139, 51904129), Basic Research Project of Yunnan Province, China (No. 202001AU070028), Basic Research Project for High-level Talents of Yunnan Province, China (No. KKS2202152011), Open Foundation of State Key Laboratory of Complex Nonferrous Metal Resources Clean Utilization, China (No. CNMRCUKF1602), and the Testing and Analyzing Funds of Kunming University of Science and Technology, China (No. 2020T20150055).

References

- [1] LIU Shuo, ZHANG Yuan-bo, SU Zi-jian, LU Man-man, GU Fo-quan, LIU Ji-cheng, JIANG Tao. Recycling the domestic copper scrap to address the China's copper sustainability [J]. *Journal of Materials Research and Technology*, 2020, 9: 2846–2855.
- [2] DONG Jing-shen, LIU Quan-jun, YU Li, SUBHONQULOV S H. The interaction mechanism of Fe^{3+} and NH_4^+ on chalcopyrite surface and its response to flotation separation of chalcopyrite from arsenopyrite [J]. *Separation Purification Technology*, 2020, 256: 117778.
- [3] DENG Jiu-shuai, WEN Shu-ming, LIU Jian, WU Dan-dan, FENG Qi-cheng. Adsorption and activation of copper ions on chalcopyrite surfaces: A new viewpoint of self-activation [J]. *Transactions of Nonferrous Metals Society of China*, 2014, 24: 3955–3963.
- [4] HEYES G W, TRAHAR W J. The natural flotability of chalcopyrite [J]. *International Journal of Mineral Processing*, 1977, 4: 317–344.
- [5] YOU K S, KIM H S, AHN J W, LEE S. Arsenic rejection from lead concentrate using aluminosulfate [J]. *International Journal of Mineral Processing*, 2013, 125: 118–121.
- [6] RINCON J, GAYDARDZHIEV S, STAMENOV L. Investigation on the flotation recovery of copper sulphosalts through an integrated mineralogical approach [J]. *Minerals Engineering*, 2019, 130: 36–47.
- [7] CHEN Jian-hua, CHEN Ye, WEI Zong-wu, LIU Feng-xia. Bulk flotation of auriferous pyrite and arsenopyrite by using tertiary dodecyl mercaptan as collector in weak alkaline pulp [J]. *Minerals Engineering*, 2010, 23: 1070–1072.
- [8] YU Li, LIU Quan-jun, LI Shi-mei, DENG Jiu-shuai, LUO Bin, LAI Hao. Depression mechanism involving Fe^{3+} during arsenopyrite flotation [J]. *Separation and Purification Technology*, 2019, 222: 109–116.
- [9] ZHANG Hui-bin, HE Yu-zheng, HU Jing-jing, WANG Ya-nan, CAO Hua-zhen, JUN ZHOU, ZHENG Guo-qu. Assessment of selective sequential extraction procedure for determining arsenic partitioning in copper slag [J]. *Transactions of Nonferrous Metals Society of China*, 2020, 30: 2823–2835.
- [10] LONG G, PENG Yong-jun, BRADSHAW D. Flotation separation of copper sulphides from arsenic minerals at Rosebery copper concentrator [J]. *Minerals Engineering*, 2014, 66/67/68: 207–214.
- [11] HUANG Guo-zhi, GRANO S, SKINNER W. Galvanic interaction between grinding media and arsenopyrite and its effect on flotation: Part II. Effect of grinding on flotation [J]. *International Journal of Mineral Processing*, 2006, 78: 198–213.
- [12] MA X, BRUCKARD W J. Rejection of arsenic minerals in sulfide flotation—A literature review [J]. *International Journal of Mineral Processing*, 2009, 93: 89–94.
- [13] YEKELER M, YEKELER H. Molecular modeling study on the relative stabilities of the flotation products for arsenic-containing minerals: Dixanthogens and arsenic(III) xanthates [J]. *Journal of Colloid and Interface Science*, 2005, 284: 694–697.
- [14] VALDIVIESO A L, SANCHEZ L A A, ESCAMILLA C O, FUERSTENAU M C. Flotation and depression control of arsenopyrite through pH and pulp redox potential using xanthate as the collector [J]. *International Journal of Mineral Processing*, 2006, 81: 27–34.
- [15] VALDIVIESO A L, ESCAMILLA C O, SONG S, BAEZ I L, MARTINEZ I G. Adsorption of isopropyl xanthate ions onto arsenopyrite and its effect on flotation [J]. *International Journal of Mineral Processing*, 2003, 69: 175–184.

- [16] CHEN Jian-hua, WANG Jin-ming, LI Yu-qiong, LIU Meng, LIU Ying-chao, ZHAO Cui-hua, CUI Wei-yong. Effects of surface spatial structures and electronic properties of chalcopyrite and pyrite on Z-200 selectivity [J]. *Minerals Engineering*, 2021, 163: 106803.
- [17] LIU Guang-yi, ZHONG Hong, DAI Tai-gen. The separation of Cu/Fe sulfide minerals at slightly alkaline conditions by using ethoxycarbonyl thionocarbamates as collectors: Theory and practice [J]. *Minerals Engineering*, 2006, 19: 1380–1384.
- [18] FILIPPI M. Oxidation of the arsenic-rich concentrate at the Prebuz abandoned mine (Erzgebirge Mts., CZ): mineralogical evolution [J]. *Science of the Total Environment*, 2004, 322: 271–282.
- [19] LATTANZI P, PELO S D, MUSU E, ATZEI D, ELSENER B, FANTAUZZI M, ROSSI A. Enargite oxidation: A review [J]. *Earth Science Reviews*, 2008, 86: 62–88.
- [20] LI G, ZHANG H. The chemical principles of flotation, activation and depression of arsenopyrite [C]//*Processing of Complex Ores*. Halifax: Elsevier, 1989: 61–70.
- [21] POLING G W, BEATTIE M J V. Selective depression in complex sulphide flotation [C]//JONES M H, WOODCOCK J T. *Principles of Mineral Flotation*. Melbourne: The Australian Institute of Mining and Metallurgy, 1984: 137–146.
- [22] BEATTIE M J V, POLING G W. Flotation depression of arsenopyrite through use of oxidizing agents [J]. *Institution of Mining and Metallurgy Transactions. Section C: Mineral Processing and Extractive Metallurgy*, 1988, 97: 15–20.
- [23] WANG Qun, HEISKANEN K. Separation of pentlandite and nickel arsenide minerals by aeration conditioning flotation [J]. *International Journal of Mineral Processing*, 1990, 29: 99–109.
- [24] GUO Xue-yi, XIN Yun-tao, HAO WANG, TIAN Qing-hua. Mineralogical characterization and pretreatment for antimony extraction by ozone of antimony-bearing refractory gold concentrates [J]. *Transactions of Nonferrous Metals Society of China*, 2017, 27: 1888–1895.
- [25] FORNASIERO D, FULLSTON D, LI C, RALSTON J. Separation of enargite and tennantite from non-arsenic copper sulfide minerals by selective oxidation or dissolution [J]. *International Journal of Mineral Processing*, 2001, 61: 109–119.
- [26] TAPLEY B, YAN D. The selective flotation of arsenopyrite from pyrite [J]. *Minerals Engineering*, 2003, 16: 1217–1220.
- [27] LI G M, ZHANG H E, USUI S. Depression of arsenopyrite in alkaline medium [J]. *International Journal of Mineral Processing*, 1992, 34: 253–257.
- [28] ABEIDU A M, ALMAHDY A M. Magnesia mixture as a regulator in the separation of pyrite from chalcopyrite and arsenopyrite [J]. *International Journal of Mineral Processing*, 1980, 6: 285–302.
- [29] ZHANG Xu, FENG Ya-li, LI Hao-ran. Enhancement of bio-oxidation of refractory arsenopyritic gold ore by adding pyrolusite in bioleaching system [J]. *Transactions of Nonferrous Metals Society of China*, 2016, 26: 2479–2484.
- [30] YANG Tao, WANG Lu, LIU Yu-lei, JIANG Jin, HUANG Zhuang-song, PANG Su-yan, CHENG Hai-jun, GAO Da-wen, MA Jun. Removal of organoarsenic with ferrate and ferrate resultant nanoparticles: Oxidation and adsorption [J]. *Environmental Science & Technology*, 2018, 52: 13325–13335.
- [31] MANOLI K, NAKHLA G, FENG M, SHARMA V K, RAY A K. Silica gel-enhanced oxidation of caffeine by ferrate(VI) [J]. *Chemical Engineering Journal*, 2017, 330: 987–994.
- [32] MUNYENGABE A, ZVINOWANDA C, ZVIMBA J N, RAMONTJA J. Innovative oxidation and kinetic studies of ferrous ion by sodium ferrate(VI) and simultaneous removal of metals from a synthetic acid mine drainage [J]. *Physics Chemistry of the Earth Parts A/B/C*, 2020, 124: 102932.
- [33] LIAO Run-peng, FENG Qi-cheng, WEN Shu-ming, LIU Jian. Flotation separation of molybdenite from chalcopyrite using ferrate(VI) as selective depressant in the absence of a collector [J]. *Minerals Engineering*, 2020, 152: 106369.
- [34] SHARMA V K. Potassium ferrate(VI): An environmentally friendly oxidant [J]. *Advances in Environmental Research*, 2002, 6: 143–156.
- [35] GAO Zhi-yong, JIANG Zhe-yi, WEI SUN, GAO Yue-sheng. Typical roles of metal ions in mineral flotation: A review [J]. *Transactions of Nonferrous Metals Society of China*, 2021, 31: 2081–2101.
- [36] MONTE M B M, DUTRA A J B, ALBUQUERQUE C R F, TONDO L A, LINS F F. The influence of the oxidation state of pyrite and arsenopyrite on the flotation of an auriferous sulphide ore [J]. *Minerals Engineering*, 2002, 15: 1113–1120.
- [37] MCKIBBEN M A, TALLANT B A, DEL ANGEL J K. Kinetics of inorganic arsenopyrite oxidation in acidic aqueous solutions [J]. *Applied Geochemistry*, 2008, 23: 121–135.
- [38] WANG Xun, LIU Jie, ZHU Yi-min, HAN Yue-xin. Adsorption and depression mechanism of an eco-friendly depressant PCA onto chalcopyrite and pyrite for the efficiency flotation separation [J]. *Colloids Surfaces A: Physicochemical Engineering Aspects*, 2021: 620: 126574.
- [39] LIU De-zhi, ZHANG Guo-fan, HUANG Gang-hong, GAO Ya-wen, WANG Meng-tao. Investigations on the selective flotation of chalcopyrite from talc using gum Arabic as depressant [J]. *Separation Science and Technology*, 2020, 55: 3438–3446.
- [40] PARK K, CHOI J, GOMEZ-FLORES A, KIM H. Flotation behavior of arsenopyrite and pyrite, and their selective separation [J]. *Materials Transactions*, 2015, 56: 435–440.
- [41] RAN Jin-cheng, QIU Xian-yang, HU Zhen, LIU Quan-jun, SONG Bao-xu, YAO Yan-qing. Enhance flotation separation of arsenopyrite and pyrite by low-temperature oxygen plasma surface modification [J]. *Applied Surface Science*, 2019, 480: 1136–1146.
- [42] YU Li, LIU Quan-jun, LI Shi-mei, DENG Jiu-shuai, LUO Bin, LAI Hao. Adsorption performance of copper ions on arsenopyrite surfaces and implications for flotation [J]. *Applied Surface Science*, 2019, 488: 185–193.
- [43] HAN Cong, WEI De-zhou, GAO Shu-ling, ZAI Qing-xiang, SHEN Yan-bai, LIU Wen-gang. Adsorption and desorption of butyl xanthate on chalcopyrite [J]. *Journal of Materials Research Technology*, 2020, 9: 12654–12660.
- [44] KHOSO S A, HU Yue-hua, LÜ Fei, GAO Ya, LIU Run-qing, SUN Wei. Xanthate interaction and flotation separation of

- H₂O₂-treated chalcopyrite and pyrite [J]. Transactions of Nonferrous Metals Society of China, 2019, 29: 2604–2614.
- [45] FANTAUZZI M, LICHERI C, ATZEI D, LOI G, ELSENER B, ROSSI G, ROSSI A. Arsenopyrite and pyrite bioleaching: Evidence from XPS, XRD and ICP techniques [J]. Analytical and Bioanalytical Chemistry, 2011, 401: 2237–2248.
- [46] LAN Zhuo-yue, LAI Zhen-ning, ZHENG Yong-xing, LV Jin-fang, PANG Jie, NING Ji-lai. Thermochemical modification for the surface of smithsonite with sulfur and its flotation response [J]. Minerals Engineering, 2020, 150: 106271.
- [47] ZHENG Xing-fu, LIU Li-zhu, NIE Zhen-yuan, YANG Yi, CHEN Jian-hua, YANG Hong-ying, XIA Jin-lan. The differential adsorption mechanism of hexahydrated iron and hydroxyl irons on a pyrite (100) surface: A DFT study and XPS characterization [J]. Minerals Engineering, 2019, 138: 215–225.
- [48] LV Jin-fang, TONG Xiong, ZHENG Yong-xing, XIE Xian, WANG Cong-bing. Study on the surface sulfidization behavior of smithsonite at high temperature [J]. Applied Surface Science, 2018, 437: 13–18.
- [49] HAN Y S, JEONG H Y, DEMOND A H, HAYES K F. X-ray absorption and photoelectron spectroscopic study of the association of As(III) with nanoparticulate FeS and FeS-coated sand [J]. Water Research, 2011, 45: 5727–5735.
- [50] FANTAUZZI M, ATZEI D, ELSENER B, LATTANZI P, ROSSI A. XPS and XAES analysis of copper, arsenic and sulfur chemical state in enargites [J]. Surface and Interface Analysis, 2006, 38: 922–930.
- [51] NASLUZOV V, SHOR A, ROMANCHENKO A, TOMASHEVICH Y, MIKHLIN Y. DFT + *U* and low-temperature XPS studies of Fe-depleted chalcopyrite (CuFeS₂) surfaces: A focus on polysulfide species [J]. The Journal of Physical Chemistry C, 2019, 123: 21031–21041.
- [52] BUCKLEY A. N, WALKER G. W. The surface composition of arsenopyrite exposed to oxidizing environments [J]. Applied Surface Science, 1988, 35: 227–240.
- [53] JIANG Tao, QIAN LI, YANG Yong-bin, LI Guang-hui, QIU Guan-zhou. Bio-oxidation of arsenopyrite [J]. Transactions of Nonferrous Metals Society of China, 2008, 18: 1433–1438.
- [54] FRAU F, ROSSI A, ARDAU C, BIDDAU R, da PELO S, ATZEI D, LICHERI C, CANNAS C, CAPITANI G C. Determination of arsenic speciation in complex environmental samples by the combined use of TEM and XPS [J]. Microchimica Acta, 2005, 151: 189–201.
- [55] YAMASHITA T, HAYES P. Analysis of XPS spectra of Fe²⁺ and Fe³⁺ ions in oxide materials [J]. Applied Surface Science, 2008, 254: 2441–2449.
- [56] LV Jin-fang, TONG Xiong, ZHENG Yong-xing, XIE Xian, HUANG Ling-yun. Reduction of Cr(VI) with a relative high concentration using different kinds of zero-valent iron powders: Focusing on effect of carbon content and structure on reducibility [J]. Journal of Central South University, 2018, 25: 2119–2130.
- [57] GALICIA P, BATINA N, GONZÁLEZ I. The relationship between the surface composition and electrical properties of corrosion films formed on carbon steel in alkaline sour medium: An XPS and EIS study [J]. Journal of Physical Chemistry B, 2006, 110: 14398–14405

高铁酸盐(VI)与毒砂表面的作用机理及其对黄铜矿与毒砂浮选分离的影响

廖润鹏^{1,2}, 胡盘金^{1,2}, 文书明^{1,2}, 郑永兴¹, 邱仙辉^{1,3}, 吕晋芳^{1,2}, 刘建^{1,2}

1. 昆明理工大学 省部共建复杂有色金属资源清洁利用国家重点实验室, 昆明 650093;
2. 昆明理工大学 国土资源工程学院, 昆明 650093;
3. 江西理工大学 资源与环境工程学院, 赣州 341000

摘要: 通过浮选试验、接触角测量、吸附量测试、交流阻抗测试和 XPS 分析研究一种新型环保抑制剂高铁酸钾(K₂FeO₄) 在乙基黄药捕收剂体系下对毒砂和黄铜矿的抑制作用。结果表明, 在 pH 值为 4~11 的范围内, 高铁酸钾强烈抑制毒砂, 在 pH 8 或 10 时, 采用 5×10⁻⁴ mol/L K₂FeO₄ 和 5×10⁻⁵ mol/L PEX 可以实现黄铜矿与毒砂的浮选分离。在 K₂FeO₄ 和 PEX 存在时, 毒砂的接触角和黄药吸附量显著降低。LEIS 测量表明, 高铁酸盐的加入可以显著增加毒砂表面的阻抗。XPS 分析进一步证实, 高铁酸盐加速毒砂表面的氧化。

关键词: 高铁酸盐(VI); 毒砂; 黄铜矿; 低碱度浮选分离

(Edited by Bing YANG)